Published in final edited form as:

Oncogene. 2017 September 07; 36(36): 5212–5218. doi:10.1038/onc.2017.141.

Cytoplasmic E3 ubiquitin ligase CUL9 controls cell proliferation, senescence, apoptosis and genome integrity through p53

Zhijun Li[1] and **Yue Xiong**[1,2]

[1]Lineberger Comprehensive Cancer Center, University of North Carolina at Chapel Hill, NC 27599, USA

[2]Department of Biochemistry and Biophysics, University of North Carolina at Chapel Hill, NC 27599, USA

Abstract

CUL9 is a member of the cullin family of E3 ubiquitin ligases, and it localizes predominantly in the cytoplasm. Deletion of *Cul9* in mice results in increased DNA damage, widespread aneuploidy, spontaneous tumor development, accelerated *Eμ-Myc*-induced lymphomagenesis, and susceptibility to carcinogenesis. CUL9 binds to p53 and causes cell apoptosis when ectopically expressed. Whether the function of CUL9 in maintaining genomic integrity and suppressing tumorigenesis is linked to p53 has not been genetically tested. Here, we report that deletion of *CUL9* in human cells results in attenuated p21 induction and impaired cellular response to DNA damage. We show that disruption of Cul9-p53 binding in mouse embryo fibroblasts (MEFs) by a knock-in mutation in Cul9 (Δp53) increases S-phase cell population, accumulates DNA damage during DNA replication, and decreases apoptosis to both endogenous and exogenous DNA-damaging agents. The extent of these alterations in $Cul9^{\Delta p53}$ MEFs is indistinguishable to those seen in $Cul9^{-/-}$ MEFs and comparable to those seen in $p53^{-/-}$ MEFs. Deletion of *CUL9* in *p53* null cells does not lead to further increase of DNA damages. Both $Cul9^{-/-}$ and $Cul9^{\Delta p53}$ MEFs proliferate faster and undergo spontaneous immortalization while retaining both Arf and p53. These results demonstrate that the functions of CUL9 in regulating cell proliferation and maintaining genomic integrity are mainly mediated by p53, and that CUL9 is a critical p53 activator.

Keywords

p53; genome stability; CUL9

Correspondence to: Yue Xiong.

Conflict of interest: The authors declare no conflict of interest.

Supplementary Information accompanies the paper on the Oncogene website (http://www.nature.com/onc)

Introduction

The tumor suppressor p53 functions to maintain genomic integrity and to suppress tumorigenesis[1]. Deletion of *p53* in mice results in spontaneous immortalization of mouse embryonic fibroblasts (MEFs) and tumorigenesis[2]. Mutations in the p53 gene are the most common genetic alterations in diverse types of human cancer[3], and in tumors retaining wildtype p53, genes involved in its regulation are frequently mutated[4]. The regulation of p53 is carried out primarily by protein modifying enzymes, and extensive biochemical and cellular studies have provided mechanisms on how these enzymes signal different stresses to p53. As each of these p53 regulatory enzymes has other non-p53 targets, one important area surrounding p53 regulation not adequately studied is the effect of disrupting the interaction between p53 and its regulators.

CUL9 belongs to the cullin family of proteins which functions as a scaffold to assemble E3 ubiquitin ligases. CUL9 (2,517 aa) is the largest and evolutionarily youngest member of the cullin family, evolving after the emergence of vertebrates[5], and it contains multiple functional domains. Two unique features of CUL9 are that it localizes predominantly in the cytoplasm and it binds to p53[6, 7]. Deletion of *Cul9* in mice results in abnormal nuclear morphology, increased DNA damage, and widespread aneuploidy in multiple tumors that develop spontaneously in multiple organ and tissues. In addition, *Cul9*$^{-/-}$ mice experience accelerated Eμ-Myc-induced lymphomagenesis and are rendered susceptible to carcinogenesis[8, 9]. Whether CUL9 plays a similarly important function in maintaining genomic integrity in human cells and how much of this function of CUL9 is dependent on p53 have not been determined.

Results

Loss of *CUL9* function reduces basal and DNA damage-induced p21 in human cells

To determine the function of CUL9 in maintaining genomic integrity in human cells, we knocked down CUL9 in human U2OS osteosarcoma cells which retain wildtype *p53* (Figure 1a). Although the steady state level of p53 did not change significantly, the basal level of the CDK inhibitor p21, a target of p53, was consistently reduced by nearly 50%. Knocking down CUL9 also reduced p21 accumulation after a low dose etoposide treatment (2 μM) by more than 50% without significantly reducing the steady state level of p53 protein (Figure 1b). To confirm these findings, we used the CRISPR-Cas9 system to delete the *CUL9* gene in U2OS cells (Figure 1c and Supplementary Figure S1a, S1a and S1c). We found that deletion of *CUL9* also resulted in reduced basal p21 level and p21 accumulation after etoposide treatment without changing the induction of the steady state level of p53 protein (Figure 1c) significantly. Together, these results demonstrate that the function of CUL9 is required for maintaining the basal and induced expression of p21 in response to DNA damage in human cells.

Loss of function of CUL9 accumulates damaged DNA and alters the cell cycle in human cells

Endogenous DNA damage occurs spontaneously during cell proliferation, representing a major source of DNA damage[10]. To determine the effect of loss of function of CUL9 on endogenous DNA damage, we stained *CUL9*-depleted or deleted U2OS cells with an antibody recognizing γ-H2AX[11]. We found that deletion of *CUL9* resulted in a significant increase (3.9-fold) of the number of γH2AX-positive cells (defined as ≥5 foci per cell), from 9.7% in parental *CUL9*+ U2OS cells to 37.9% in *CUL9*-KO U2OS cells (Figure 1d). Moreover, the number of γH2AX foci in the γH2AX-positive cells was also significantly increased by *CUL9* deletion (2.3-fold), from an average of 7.9 per cell in parental *CUL9*+ U2OS cells to 18.2 in *CUL9*-KO U2OS cells. The same result was obtained in U2OS cells after CUL9 knockdown which increased both γH2AX-positive cells, from 11.6% in control U2OS cells to 26.2% in CUL9-depleted U2OS cells (2.3-fold, Supplementary Figure S1d), and the number of γH2AX foci in the γH2AX-positive cells, from an average of 5.8 foci per cell in control cells to 12.5 in CUL9-depleted U2OS cells (2.2-fold).

Deletion of *CUL9* in *p53* null cells does not further increase of endogenous DNA damages

To determine the genetic interaction between *CUL9* and *p53* in suppressing endogenous DNA damage, we deleted *p53* in both parental and *CUL9*-KO U2OS cells (referred to as *p53*-KO and *p53-CUL9* DKO, respectively, Figure S1e) and determined the endogenous DNA damage in these cells by γ-H2AX staining. We found that deletion of *p53* resulted in a significant increase of the number of γH2AX-positive cells (3.1-fold), from 11.9% in parental *p53*+ U2OS cells to 36.5% in *p53*-KO U2OS cells (Figure 1e). The number of γH2AX foci per individual γH2AX-positive cell was also significantly increased in *p53*-KO U2OS cells by 2.1-fold, from an average of 8.8 γH2AX foci per cell in parental *p53*+ U2OS cells to 18.1 foci in *p53*-KO U2OS cells. Notably, the increases in both γ-H2AX foci and number of γH2AX foci per cells caused by *p53* deletion were similar to *CUL9* deletion. Importantly, the percentage of γ-H2AX positive in *p53-CUL9* DKO U2OS cells (35.7%) was similar to those detected in either *p53*-KO cells (36.5%) and slightly higher than those accumulated in *CUL9*-KO cells (31.5%) (Figure 1e). These results demonstrates that deletion of *CUL9* in p53 null cells does not further increase DNA double strand breaks, supporting the notion that the function of CUL9 in preventing endogenous DNA damage is mediated primarily by p53.

Loss of function of CUL9 impairs cellular response to exogenous DNA damaging agent

Flow cytometry analysis showed that *CUL9* depletion slightly increased the proportion of S-phase cells as compared with control cells, from 16.4% to 17.7%, in the absence of exogenous DNA-damaging agent, but resulted in a significant (2.0- and 2.4-fold) increase of S-phase cells after 24 hours of treatment with either 2.5 μM or 5.0 μM etoposide, respectively (Figure 1f). Deletion of *CUL9* resulted in a more pronounced increase (72%) of S-phase cells, from 9.4% to 16.2% in the absence of an exogenous DNA damage agent, and an even more significant (3.5-fold) increase of S-phase cells than *CUL9*-depleted U2OS cells after being exposed to 5 μM etoposide for 24 hours, from 12% to 42.5% (Figure 1g). The increase of S-phase cells after *CUL9* depletion was accompanied by a reduction of the

G1 cell population. There was a clear decrease in the sub-G1 cell population in *CUL9*-KO cells when compared to control *CUL9*+ U2OS cells, from 4.9% to 1.8% (2.7-fold) in the absence of exogenous DNA damage and from 6.0% to 2.5% (2.4-fold) after etoposide treatment. Together, these results demonstrate that loss of CUL9 function, like loss of p53 function, alters cell cycle control and impairs DNA damage response to both endogenous and exogenous DNA-damaging agents.

Disruption of Cul9-p53 binding impairs cellular response to DNA damage

We previously identified several single amino acid substitutions in the p53-binding region of human CUL9, including Q417A, that disrupts its binding with p53[12]. To determine whether the function of CUL9 in maintaining genomic integrity is linked to p53, we knocked in a mutation to the mouse *Cul9* gene—Q418A (equivalent to human Q417A substitution)—in ES cells and derived both heterozygous and homozygous mutant MEFs (referred to as $Cul9^{\Delta p53/+}$ and $Cul9^{\Delta p53/\Delta p53}$, respectively). We verified that this mutation, like its human homologous Q417A mutation, almost disrupted Cul9-p53 binding completely, without any significant effect on the binding of Cul9 with Roc1 (Figure 2a). Like deletion of *Cul9* in MEF (Supplementary Figure S2a), disruption of Cul9's binding with p53 resulted in decreased and delayed p53 phosphorylation on Ser15 and reduced accumulation of p53 and p21 protein (Figure 2b). These results indicate that Cul9 regulates p21 through p53 that Cul9. Accumulation of Ser15-phosphorylated p53 in $Cul9^{\Delta p53/\Delta p53}$ MEFs following etoposide suggests that Cul9, although affecting p53 level in MEFs, does not play a direct role in regulation of Ser15 phosphorylation of p53. Disruption of Cul9's binding with p53 had no detectable effect on the steady state level of survivin, a substrate of Cul9 E3 ligase[8], suggesting that Cul9-p53 binding is not required for the regulation of survivin ubiquitylation by Cul9.

Disruption of p53 binding in Cul9 resulted in a significant increase (4.95-fold) of γH2AX-positive cells, from 8.5% in wild-type MEFs to 42.1% in $Cul9^{\Delta p53/\Delta p53}$ MEFs (Figure 2c). Likewise, the number of γH2AX foci in the γH2AX-positive cells was significantly increased (1.9-fold) by the disruption of Cul9-p53 binding, from an average of 8.9 foci per positive cell in wild-type MEFs to 17.3 in $Cul9^{\Delta p53/\Delta p53}$ MEFs. Deletion of *p53* also resulted in a significant increase of both the percentage of γH2AX-positive cells (by 5.35-fold) and the number of γH2AX foci in the γ-H2AX-positive cells (by 2.22-fold), from 9.4% γH2AX-positive cells and 8.5 γH2AX foci per γ-H2AX-positive cell in *p53* wild-type MEFs to 50.3% and 18.9 in $p53^{-/-}$ MEFs, respectively (Figure 2d). Both increases of the percentage of γH2AX-positive cells and the number of γH2AX foci in each cell seen in $Cul9^{\Delta p53/\Delta p53}$ MEFs were comparable to those seen in $p53^{-/-}$ MEFs, suggesting that Cul9 plays a major role in signaling p53 in the maintenance of genomic integrity. Supporting a major role of Cul9 in signaling to p53, the p21 level was reduced similarly in $Cul9^{\Delta p53/\Delta p53}$ MEFs as in $p53^{-/-}$ MEFs when compared to wildtype MEFs (Figure 2b and 2c).

To determine the genetic interaction between *CUL9* and *p53* in suppressing endogenous DNA damage in MEFs, we generated p53-Cul9 double knockout (DKO) MEFs (Supplementary Figure S2b) and determined endogenous DNA damage by γH2AX staining. We found that both the percentage of γ-H2AX positive cells and the number of γH2AX foci

per cells in *p53-Cul9* DKO MEFs (44.7% and 19.9 γH2AX foci per cell) were similar to those detected in either *p53* MEFs (43.5% and 21.1 foci per cell), but were somewhat higher than those detected in the *Cul9* MEFs (39.2% and 18.6 foci per cell) (Figure 2e). These results support the notion that the function of CUL9 in preventing endogenous DNA damage is mediated most by p53 in MEFs, as is the case in U2OS cells.

Disruption of Cul9-p53 binding accumulates DNA damage during replication and reduces apoptosis

In human U2OS cells, depletion or deletion of CUL9 results in a significant increase of S-phase cell population and a decrease in the sub-G1 cell population (Figure 1). To probe the link between the function of CUL9 in maintaining genomic integrity and in cell cycle checkpoint control, we determined when the spontaneous DNA damage occurred in the cell cycle and how this is affected by the disruption of Cul9-p53 binding. We pulse-labelled exponentially-growing cells for 30 minutes with 5-ethynyl-2′-deoxyuridine (EdU), a thymidine analogue, and identified cells undergoing active DNA synthesis using a fluorescent azide to detect incorporated EdU [13] and DNA damage using γH2AX antibody. EdU-positive cells were increased from 14.2% in wildtype MEFs to 26.7% in *Cul9*$^{\Delta p53/\Delta p53}$ MEFs, 32.3% in *Cul9*$^{-/-}$ MEFs and 37.4% in *p53*$^{-/-}$ MEFs (Figure 3a), indicating a significant increase of the S-phase cell population by the deletion of *p53* or *Cul9*, or the disruption of Cul9-p53 binding with loss of p53 being the most potent in stimulating DNA replication. The percentage of γH2AX-positive cells was increased from 13.9% in wildtype MEFs to 30.7% in *Cul9*$^{\Delta p53/\Delta p53}$ MEFs, 29.2% in *Cul9*$^{-/-}$ MEFs and 36.5% in *p53*$^{-/-}$ MEFs, indicating a significant increase of DNA damage by either the deletion of *p53* or *Cul9* or the disruption of Cul9-p53 binding. Compared to the wildtype MEFs which had 14.2% EdU- and 14.9% γH2AX-positive cells, *Cul9*$^{\Delta p53/\Delta p53}$ and *Cul9*$^{-/-}$ MEFs had similar increases in S-phase population (26.7% vs 29.2%) and γH2AX-positive cells (29.3% vs 32.3%), suggesting that the functions of Cul9 in preventing the accumulation of endogenous DNA damage and regulating cell cycle are largely dependent upon its binding with p53. Almost all γH2AX-positive cells were also positive for EdU in wildtype (95.3%), *Cul9*$^{\Delta p53/\Delta p53}$ (91.1%), *Cul9*$^{-/-}$ (90.4%) and *p53*$^{-/-}$ (97.6%) MEFs, indicating that nearly all spontaneous DNA damage occurred during DNA replication in wildtype MEFs and was substantially exacerbated by the loss of *p53* or *Cul9* or the disruption of Cul9-p53 binding. In contrast to wildtype MEFs, *p53*$^{-/-}$, *Cul9*$^{-/-}$, and *Cul9*$^{\Delta p53/\Delta p53}$ MEFs all had substantially reduced apoptosis in the absence of adding a DNA-damaging agent exogenously or post- etoposide treatment, as determined by flow cytometric TUNEL analysis (Figure 3b and Supplementary Figures S3a and S3b). Notably, the extent of the suppression of apoptosis was very similar between the three mutant MEF lines. Taken together, these results support the notion that Cul9 plays a significant role in controlling the function of p53, which in turn regulates the cell cycle checkpoint, apoptosis and maintained genome integrity.

Disruption of Cul9-p53 binding increases the rate of MEF cell proliferation and causes MEF spontaneous immortalization

Cul9$^{\Delta p53/\Delta p53}$ MEFs were morphologically normal, but appeared to be proliferating at a faster rate as shown by higher cell density (Figure 4a). Indeed, when compared to wildtype MEF, heterozygous *Cul9*$^{\Delta p53/+}$ MEFs proliferated at a higher rate and the homozygous

Cul9$^{\Delta p53/\Delta p53}$ MEFs proliferated even faster (Figure 4b). Surprisingly, when assayed on a 3T9 proliferation and immortalization protocol[14], three independently derived *Cul9*$^{\Delta p53/\Delta p53}$ MEF lines underwent spontaneous immortalization, as did *Cul9*$^{-/-}$ MEFs. In contrast, wild-type MEFs ceased proliferating around passage 10 (Figure 4c). *p53* and *Arf*, an inhibitor of MDM2 and an activator of p53, play the major role in maintaining MEF cellular senescence. Wildtype MEFs can escape senescence at a very low frequency, and MEF variants that rarely immortalize spontaneously usually sustain a mutation in either p53[15] or Arf[16], an inhibitor of MDM2 and an activator of p53. Deletion of either p53 or Arf or both *p53* and *Cul9* gene, as expected, resulted in MEFs spontaneous immortalization (Figure 4c). Notably, in immortalized *Cul9*$^{\Delta p53\Delta p53}$ or *Cul9*$^{-/-}$ MEFs spontaneously, both p53 and Arf were retained and expressed at levels similar to wildtype MEFs (Figure 4d). This result indicates that deletion of *Cul9* or disruption of Cul9-p53 binding releases the selection pressure to lose either p53 or Arf during cellular immortalization. We noted that both *Cul9*$^{\Delta p53/\Delta p53}$ and *Cul9*$^{-/-}$ MEFs proliferated at a slower rate compared with either *p53*$^{-/-}$ and *Arf*$^{-/-}$ MEFs and that *p53*$^{-/-}$;*Cul9*$^{-/-}$ DKO MEFs proliferated at a rate that is indistinguishable from that seen in *p53*$^{-/-}$ MEF (Figure 4c). This result supports the notion that the function of Cul9 in regulating cell proliferation is primarily mediated by p53 and also suggests that p53 has additional, Cul9-independent activity in regulating cell proliferation.

Discussion

Many p53 modifying enzymes have been extensively characterized [17], and the most widely studied p53 modifying enzymes are MDM2 and MDMX E3 ubiquitin ligases. Deletion of either *Mdm2* or *Mdmx/Mdm4* results in mouse embryonic lethality which can be rescued by the co-deletion of *p53*[18-20], and p53 has been established as the main functional target of both genes during early development. The roles of p53 as the downstream effector of other p53 modifying enzymes are yet to be genetically determined, however. The main finding of this report is that the function of CUL9 in maintaining genomic integrity is primarily, if not entirely mediated by p53. This is based on the quantitative measurement of three functions —G1-to-S transition, apoptosis and DNA damage—known to be mediated by p53, and it is derived from genetic studies from tumor-derived human cells, as well as primary MEFs. Notably, these alterations in *Cul9* null and *Cul9*$^{\Delta p53}$ MEFs are comparable to those seen in *p53* null MEFs, suggesting, conversely, that CUL9 plays a significant role in signaling DNA damage and G1 checkpoint to p53. Nearly a dozen ubiquitin ligases have been implicated in the regulation of p53, all promoting p53 degradation and thereby negatively regulating the function of p53[21]. CUL9 is thus far the only ubiquitin ligase that has been genetically linked to p53 activation. The detailed mechanism by which CUL9 activates p53 is currently unknown. Although both deletion of *CUL9* and disruption of Cul9-p53 binding consistently reduced the basal and induced p21 protein level after exposing cells to exogenous DNA-damaging agent in U2OS and MEF cells, the steady state level of p53 protein was appreciably reduced in *Cul9* null and *Cul9*$^{\Delta p53}$ MEFs, but not in U2OS cells depleted or deleted for *CUL9*. It is not clear at present whether this disparity reflects a difference between human and mouse, or between tumor-derived and primary cells. Lack of significant change in p53 protein level in U2OS cells after losing CUL9 function suggests that CUL9 could activate p53 through a mechanism that is not dependent upon stabilizing p53 protein.

It will be important for future studies to determine biochemically how the ubiquitin ligase function and cytoplasmic localization of CUL9 lead to p53 activation.

Supplementary Material

Refer to Web version on PubMed Central for supplementary material.

Acknowledgments

We thank Hui Xiao Chao, Jeremy Purvis and Matthew Smith for reading the manuscript, Dale Ramsden for discussion throughout this study, and members of the Xiong laboratory for helpful discussions and encouragement. This work was supported by National Institutes of Health grant R01CA068377 to Y. X. and a Team Innovation Award by the UNC Lineberger Comprehensive Cancer Center's University Cancer Research Fund.

References

1. Lane D, Levine A. p53 Research: the past thirty years and the next thirty years. Cold Spring Harb Perspect Biol. 2010; 2:a000893. [PubMed: 20463001]
2. Donehower LA, Lozano G. 20 years studying p53 functions in genetically engineered mice. Nat Rev Cancer. 2009; 9:831–841. [PubMed: 19776746]
3. Hollstein M, Sidransky D, Vogelstein B, Harris CC. p53 mutations in human cancers. Science. 1991; 253:49–53. [PubMed: 1905840]
4. Stracquadanio G, Wang X, Wallace MD, Grawenda AM, Zhang P, Hewitt J, et al. The importance of p53 pathway genetics in inherited and somatic cancer genomes. Nat Rev Cancer. 2016; 16:251–265. [PubMed: 27009395]
5. Marin I. Diversification of the cullin family. BMC Evol Biol. 2009; 9:267. [PubMed: 19925652]
6. Andrews P, He YJ, Xiong Y. Cytoplasmic localized ubiquitin ligase cullin 7 binds to p53 and promotes cell growth by antagonizing p53 function. Oncogene. 2006; 25:4534–4548. [PubMed: 16547496]
7. Nikolaev AY, Li M, Puskas N, Qin J, Gu W. Parc: a cytoplasmic anchor for p53. Cell. 2003; 112:29–40. [PubMed: 12526791]
8. Li Z, Pei XH, Yan J, Yan F, Cappell KM, Whitehurst AW, et al. CUL9 mediates the functions of the 3M complex and ubiquitylates survivin to maintain genome integrity. Mol Cell. 2014; 54:805–819. [PubMed: 24793696]
9. Yan J, Yan F, Li Z, Sinnott B, Cappell KM, Yu Y, et al. The 3M complex maintains microtubule and genome integrity. Mol Cell. 2014; 54:791–804. [PubMed: 24793695]
10. Vilenchik MM, Knudson AG. Endogenous DNA double-strand breaks: production, fidelity of repair, and induction of cancer. Proc Natl Acad Sci U S A. 2003; 100:12871–12876. [PubMed: 14566050]
11. Rogakou EP, Boon C, Redon C, Bonner WM. Megabase chromatin domains involved in DNA double-strand breaks in vivo. J Cell Biol. 1999; 146:905–916. [PubMed: 10477747]
12. Pei XH, Bai F, Li Z, Smith MD, Whitewolf G, Jin R, et al. Cytoplasmic CUL9/PARC ubiquitin ligase is a tumor suppressor and promotes p53-dependent apoptosis. Cancer Res. 2011; 71:2969–2977. [PubMed: 21487039]
13. Salic A, Mitchison TJ. A chemical method for fast and sensitive detection of DNA synthesis in vivo. Proc Natl Acad Sci U S A. 2008; 105:2415–2420. [PubMed: 18272492]
14. Sharpless, NE. Preparation and immortlization of primary murine cells. In: Celis, JE., editor. Cell Biology (Third Edition): A laboratory handbook. Vol. 1. 2006. p. 223-228.
15. Harvey DM, Levine AJ. p53 alteration is a common event in the spontaneous immortalization of primary BALB/c murine embryo fibroblasts. Genes Dev. 1991; 5:2375–2385. [PubMed: 1752433]
16. Kamijo T, Zindy F, Roussel MF, Quelle DE, Downing JR, Ashmun RA, et al. Tumor suppression at the mouse INK4a locus mediated by the alternative reading frame product p19ARF. Cell. 1997; 91:649–659. [PubMed: 9393858]

17. Meek DW, Anderson CW. Posttranslational modification of p53: cooperative integrators of function. Cold Spring Harb Perspect Biol. 2009; 1:a000950. [PubMed: 20457558]
18. Montes de Oca Luna R, Wagner DS, Lozano G. Rescue of early embryonic lethality in mdm2-deficient mice by deletion of p53. Nature. 1995; 378:203–206. [PubMed: 7477326]
19. Jones SN, Roe AE, Donehower LA, Bradley A. Rescue of embryonic lethality in Mdm2-deficient mice by absence of p53. Nature. 1995; 378:206–208. [PubMed: 7477327]
20. Parant J, Chavez-Reyes A, Little NA, Yan W, Reinke V, Jochemsen AG, et al. Rescue of embryonic lethality in Mdm4-null mice by loss of Trp53 suggests a nonoverlapping pathway with MDM2 to regulate p53. Nat Genet. 2001; 29:92–95. [PubMed: 11528400]
21. Pant V, Lozano G. Limiting the power of p53 through the ubiquitin proteasome pathway. Genes Dev. 2014; 28:1739–1751. [PubMed: 25128494]

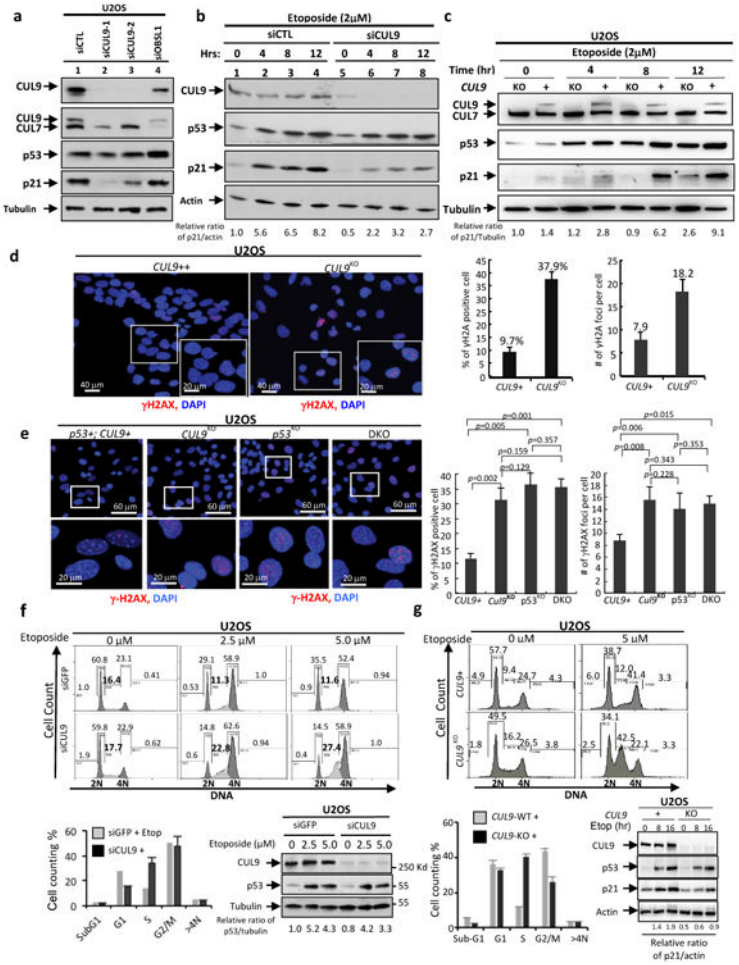

Figure 1. Loss of CUL9 function impairs cellular response to DNA damage in human cells

(**a, b**). U2OS cells were transfected with indicated siRNAs for 72 hours, either untreated (a) or treated with etoposide (2 μM) for indicated length of time presence (b). U2OS cells were cultured in McCoy's 5A with 10% FCS and incubated at 37°C, 5% CO_2. All siRNA oligos were purchased commercially from Invitrogen. siRNA, Stealth RNAi™ siRNA Negative Controls LO GC (12935-200) was used as negative control. The siRNA oligo sequences for CUL9 are: siCUL9-1: GCUGAGAGACACGUUGUUUAG; siCUL9-2: GCUGAAUAAAGGUCUCUUUCU siCUL9-3:UACUGAGGGUGCUCUUCUG. U2OS cells cultured on a 6-well plate at 30–40% confluency were transfected with Oligofectamine per the manufacturer's protocol (Invitrogen) and analyzed 48-72h after transfection. Cell extracts were subjected to immunoblot with indicated antibodies. Data in (**b**) are presented as means ± SD of three independents. (**c**) Parental *CUL9*+ and *CUL9* deleted U2OS cells were treated with 2 μM etoposide for indicated lengths of time. The expressions of proteins were determined by immunoblot analysis. (**d, e**) Parental (*p53*+, *CUL9*+), *CUL9*-KO, *p53*-KO and *p53*-*CUL9* DKO U2OS cells were stained with γH2AX antibody antibody (1:500) (9718S; Cell Signaling Technology), and DAPI. A representative view is shown on the left. Quantifications are shown on the right. 308 *CUL9*+ and 285 *CUL9*-KO cells were examined, respectively for (d), and 198 parental (*p53*+, *CUL9*+), 211 *CUL9*-KO, 253 *p53*-

KO and 209 *p53-CUL9* DKO cells were examined for (e). Cells grown in MatTek glass bottom dishes were fixed for 10 min in PBS containing 4% paraformaldehyde, washed twice with PBS, permeabilized in 0.05% Triton-X at 4 degrees for five minutes, washed once and blocked in 2% BSA for 30 min. Cells were incubated with primary antibody in PBS/BSA for >2 hr, washed and stained with appropriate fluorescent-conjugated antibody (Jackson ImmunoResearch Laboratories) for 90 min. Cells were examined with an Olympus inverted microscope with fluorescence illumination source or FV1000 confocal system. The γ-H2AX foci were analyzed using ImageJ (by NIH Image). The photographs shown are representative for each experiment. (**f**) Cells were harvested at 24 h after drug treatment and stained with propidium iodide, followed by flow cytometry analysis. Each panel represents the analysis of 20,000 events (cells). Data are presented as means ± SD of three independent tests. (**g**) $CUL9^{+}$ and $CUL9^{KO}$ U2OS cell were treated with either solvent DMSO or etoposide, followed by flow cytometry. Data are presented as means ± SD of three independent tests. For cell cycle analysis, after trypsinization and PBS wash, cells were fixed by cold ethanol for at least 3 hours. Total DNA was stained by PI (P4170; Sigma).

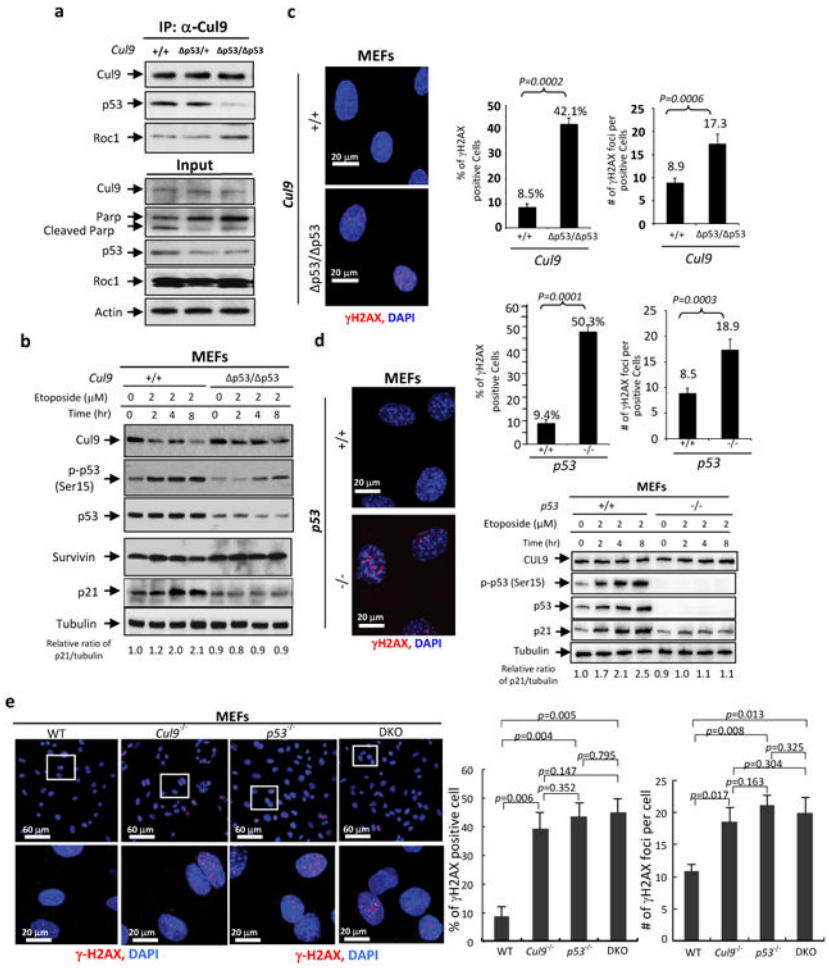

Figure 2. Disruption of Cul9-p53 binding impairs cellular response to DNA damage

(**a**) Disruption of Cul9-p53 binding by the Q418A mutation is verified by IP-western analysis. (**b**) Wild-type and *Cul9*$^{\Delta p53/\Delta p53}$ MEFs were exposed to etoposide for indicated length of time, followed by western blotting. MEFs were maintained in DMEM with 10% FCS; all cells were incubated at 37°C, 5% CO_2. (**c, d**) Wild-type, *Cul9*$^{\Delta p53/\Delta p53}$ and *p53*$^{-/-}$ MEFs were stained with γ-H2AX antibody and DAPI. A representative view is shown on the left. Quantification of γ-H2AX-positive cells were scored from 200 WT and 164 *Cul9*$^{\Delta p53/\Delta p53}$ MEF cells for (d), and 204 WT and 197 *p53*$^{-/-}$ MEF cell for (d). (**e**) Wild-type, *Cul9*$^{-/-}$, *p53*$^{-/-}$ and *Cul9*$^{-/-}$; *p53*$^{-/-}$ DKO MEFs were stained with γ-H2AX antibody and DAPI. A representative view is shown on the left. Quantification of γ-H2AX-positive cells were scored from 169 WT, 196 *Cul9*$^{-/-}$, 264 *p53*$^{-/-}$ and 287 *Cul9*$^{-/-}$;*p53*$^{-/-}$ DKO MEF cells.

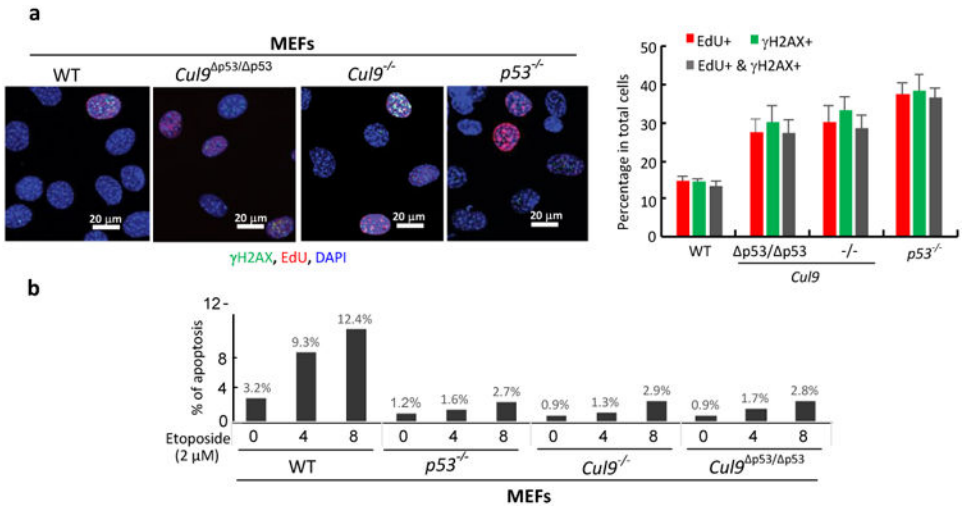

Figure 3. Disruption of Cul9-p53 binding accumulates DNA damage during S-phase and reduces apoptosis

(**a**) MEFs of indicated genotype were pulsed with EdU for 30 min, fixed and stained with DAPI and antibody recognizing γ-H2AX and EdU. A representative view is shown on the left. Quantification of the percentage of EdU-positive, γ-H2AX-positive, and EdU, γ-H2AX double positive cells were scored microscopically from 214 *Cul9*$^{\Delta p53/\Delta p53}$, 257 *Cul9*$^{-/-}$ and 271 *p53*$^{-/-}$MEF cells. For simultaneous detecting DNA replication and damage, cells were seeded, grown overnight and then were pulsed with EdU for 30 min. Cells were then fixed in 4% paraformaldehyde in phosphate buffered saline (pH 7.4; PBS). The EdU positive cells were detected using the fluorescent azide probe (Lumiprobe), followed by immunofluorescence labelling 13. Cells were blocked and permeabilized with 2% BSA in PBS for 1 hour and then incubated in γ-H2AX primary antibody (Cell Signaling, 1:500) for 2-3 hours. Cells were then incubated with secondary antibody for 1 hour at room temperature, after 3 times wash, the cells were stained with DAPI to visualize the nuclei. Cells were examined with an Olympus inverted microscope with fluorescence illumination source or FV1000 confocal system. For each EdU experiment, multiple randomly selected fields were imaged and the numbers EdU positive cells and the γ-H2AX foci were analyzed using ImageJ (by NIH Image). (**b**) Untreated and etoposide-treated MEFs of different genotypes were stained with Annexin V and PI, followed by flow cytometric analysis. Quantifications of total apoptosis are shown. For apoptosis or cell death analysis, cells were harvested by trypsinization, stained with Annexin V–7AAD and then analyzed by FACS. FACS analysis was performed using the CYAN ADP Analyzer (Dako, Fort Collins, Colorado). Data analysis was performed using Summit v4.3 software (Dako).

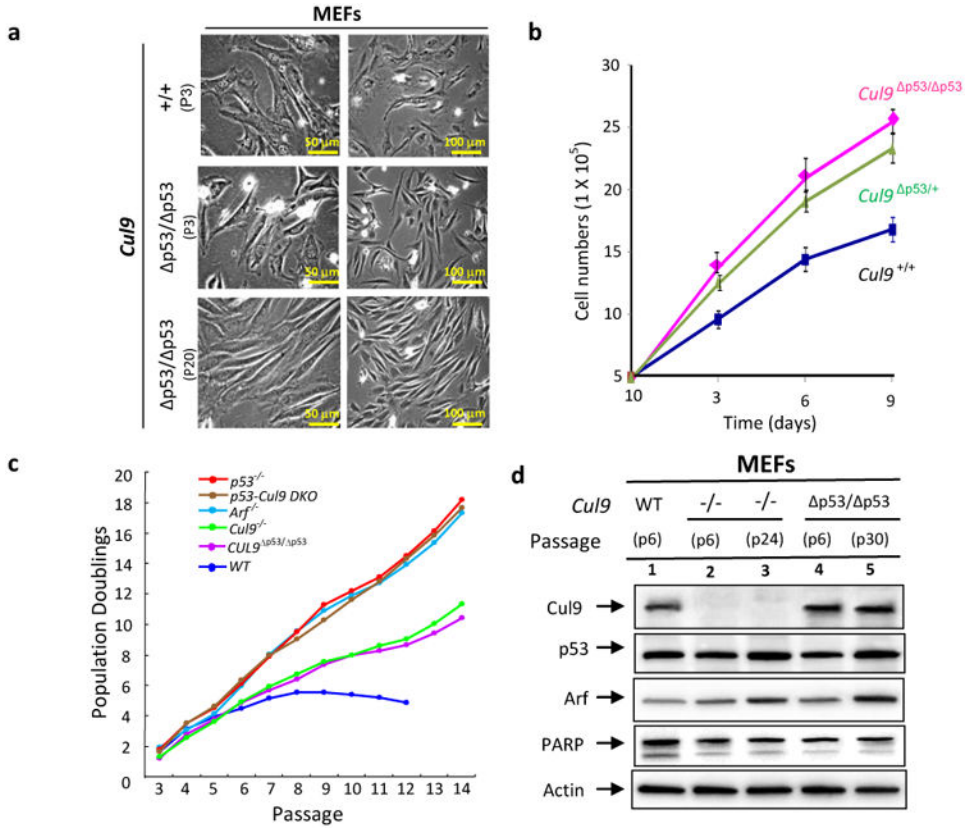

Figure 4. Disruption of Cul9-p53 binding increases the rate of MEF cell proliferation and causes MEF spontaneous immortalization

(**a**) Morphological comparison of wildtype and *Cul9*$^{QA/QA}$ MEFs at early and late passages. (**b**) 5×10^5 early passage (P3) MEFs of different genotypes were seeded and cell numbers counted over a period of 9 days. (**c**) MEFs with indicated genotypes were passaged in vitro on defined 3T9 protocol. Growth curves of MEFs at early passage (< passage 4) were determined by plating 2×103 cells in 35 mm diameter dishes; duplicate cultures were harvested every day thereafter and cells were counted. Serial cultures were done according to the 3T9 protocol. Briefly, 1×10^6 cells were plated on a 100-mm dish in DMEM/10% FBS, and cell numbers were counted after three days of culture. 1×10^6 cells were plated again and the procedure was repeated for 20 passages. For cell cycle analysis, early passage MEFs (< passage 4) from individual embryos were plated in 100-mm plates and incubated in DMEM plus 10% FBS for 24 h. (**d**) Total cell extracts were prepared from wildtype and mutant MEF at early passage or after immortalization. The levels of individual proteins were determined by western blotting with indicated antibodies.